European Journal of Pharmaceutical Sciences 181 (2023) 106361

Contents lists available at ScienceDirect

European Journal of Pharmaceutical Sciences

journal homepage: www.elsevier.com/locate/ejps

Development and validation of a porcine artificial colonic mucus model reflecting the properties of native colonic mucus in pigs

Vicky Barmpatsalou [a], Agnes Rodler [a,b], Magdalena Jacobson [c], Eva Marie-Louise Karlsson [d], Betty Lomstein Pedersen [e], Christel Anna Sofie Bergström [a,*]

[a] The Swedish Drug Delivery Center, Department of Pharmacy, Uppsala University, Box 580, SE-751 23, Uppsala, Sweden
[b] The Swedish Drug Delivery Center, Department of Medicinal Chemistry, Uppsala University, Box 574, SE-751 23, Uppsala, Sweden
[c] Department of Clinical Sciences, Faculty of Veterinary Medicine and Animal Sciences, Swedish University of Agricultural Sciences, Box 7054, SE-750 07, Uppsala, Sweden
[d] Oral Product Development, Pharmaceutical Technology & Development, Operations, AstraZeneca, Gothenburg, Sweden
[e] Product Development & Drug Delivery, Global Pharmaceutical R&D, Ferring Pharmaceuticals A/S, Amager Strandvej 405, Kastrup 2770, Denmark

A B S T R A C T

Colonic mucus plays a key role in colonic drug absorption. Mucus permeation assays could therefore provide useful insights and support rational formulation development in the early stages of drug development. However, the collection of native colonic mucus from animal sources is labor-intensive, does not yield amounts that allow for routine experimentation, and raises ethical concerns. In the present study, we developed an *in vitro* porcine artificial colonic mucus model based on the characterization of native colonic mucus. The structural properties of the artificial colonic mucus were validated against the native secretion for their ability to capture key diffusion patterns of macromolecules in native mucus. Moreover, the artificial colonic mucus could be stored under common laboratory conditions, without compromising its barrier properties. In conclusion, the porcine artificial colonic mucus model can be considered a biorelevant way to study the diffusion behavior of drug candidates in colonic mucus. It is a cost-efficient screening tool easily incorporated into the early stages of drug development and it contributes to the implementation of the 3Rs (refinement, reduction, and replacement of animals) in the drug development process.

1. Introduction

The gastrointestinal (GI) mucus is a complex hydrogel that forms a dense layer covering the luminal side of the GI epithelium (Atuma et al., 2001). It plays a key role in protecting the sensitive epithelial cells from the noxious intraluminal contents in the gastrointestinal tract (GIT), by restricting the passage of foreign particles and pathogens (Brieland et al., 2001; Lindén et al., 2002). The biophysical barrier properties of the mucus derive from its chemical and mechanical characteristics. As a biological hydrogel, it has a high water content (83-86%) (Larhed, Artursson, and Björk, 1998) and its main structural components are the mucins. These consist of a densely glycosylated protein backbone (Carlstedt and Sheehan, 1984). These complex oligosaccharide structures result in the characteristic "brush-like" configuration of the mucins. Additionally, the mucins contain non-glycosylated, hydrophobic regions involved in the self-assembly, stabilization, and crosslinking of the mucins (Ambort et al., 2011; Ambort et al., 2012).

The wide variety of structural domains in the mucins provide multiple binding sites. These enable a plethora of potential physicochemical interactions, such as hydrogen bonding, and electrostatic and hydrophobic interactions with diffusing molecules (Sigurdsson, Kirch, and Lehr, 2013; Iqbal et al., 2012). Proteins, lipids, ions, DNA, cells, and cellular debris are also present in the GI mucus (Bansil and Turner, 2006; Thornton and Sheehan, 2004; Button et al., 2013; Carlstedt and Sheehan, 1989), providing other potential binding partners and further contributing to the physicochemical barrier characteristics of the mucus. From a structural perspective, the mucins have the ability to organize themselves as dimers and trimers, resulting in a characteristic complex heterogeneous mesh network with viscoelastic properties (Lai et al., 2009). The dynamic mucin gel network is responsible for the size-exclusion filtering properties of the mucus by which it hinders the passage of particulates and bacteria larger than the mucin mesh (Cone, 2009; Perez-Vilar and Hill, 1999).

From a drug delivery point of view, the selective permeability of the mucus also extends to diffusing drug molecules (Larhed, Artursson, and Björk, 1998; Bhat, Flanagan, and Donovan, 1996; Larhed et al., 1997; Yildiz et al., 2015). As research findings elucidate the impact of the GI mucus on drug absorption, the mucus barrier needs to be taken into account in drug candidate screening and formulation development/optimization. For this reason, there is an increased interest in

* Corresponding author.
E-mail address: christel.bergstrom@farmaci.uu.se (C.A.S. Bergström).

https://doi.org/10.1016/j.ejps.2022.106361
Received 30 August 2022; Received in revised form 12 December 2022; Accepted 13 December 2022
Available online 14 December 2022
0928-0987/© 2022 The Authors. Published by Elsevier B.V. This is an open access article under the CC BY-NC-ND license (http://creativecommons.org/licenses/by-nc-nd/4.0/).

mimicking the mucus barrier *in vitro*, to increase the biorelevance and predictive power of preclinical assessments.

Several approaches exist to represent the mucus barrier in a laboratory setting, with ranging degrees of complexity and predictive power (Wright et al., 2021). Solutions of reconstituted lyophilized commercial mucin of either porcine stomach or bovine submaxillary gland origin are widely used in mucus permeation studies, mainly due to commercial accessibility and simple preparation protocols (Sardelli et al., 2019). However, the purification process of commercial mucins disrupts their gel-forming properties, resulting in rheological profiles that do not match the ones of native mucus in physiologically relevant concentrations (Kocevar-Nared, Kristl, and Smid-Korbar, 1997). Additionally, key components of the mucus, such as proteins and lipids, are removed leading to an underestimation of the mucus binding potential.

Native mucus excised from laboratory animal tissue might be considered the gold standard for mucus permeation studies, as it allows the representation of all key mucus components. However, there are practical and ethical considerations related to the collection of native mucus. First, the collection is a time-sensitive procedure in order to prevent degradation of the mucus, and improper handling can result in contamination with epithelial cells. Second, non-harmonized mucus collection protocols result in high variability in the sampling (Macierzanka, Mackie, and Krupa, 2019). Third, the collection of native mucus is tedious and labor-intensive. Especially in the large intestine, where the mucus adheres tightly to the epithelium, the collection might not yield adequate amounts for routine experimentation (Barmpatsalou et al., 2021). Given that the samples are of biological source, proper disinfection protocols should be in place, often accompanied by an additional cost. Finally, the collection of native mucus is dependent on animal availability, which is not in accordance with the 3R recommendations for the refinement, reduction, and replacement of animal models in preclinical assessments.

Other approaches to mimic the mucus barrier involve mucus-secreting cell lines, such as the methotrexate-treated HT29 cell line (HT29-MTX). These cells are often co-cultured with Caco-2 cells, because the latter mimic intestinal enterocytes. The resulting co-culture allows simultaneous assessment of mucus diffusion and cellular uptake. However, the thickness of the secreted mucus varies substantially and may depend on the growth environment (Navabi, McGuckin, and Lindén, 2013). Additional hurdles, such as the necessity of proper infrastructure for cell handling, trained personnel, and the associated costs of long cultivation periods, limit the usefulness of such mucus-secreting co-cultures in the early stages of drug candidate screening. Consequently, focus has shifted towards bio-inspired mucus models that would capture the key mucus properties, be easily prepared in the laboratory at relatively low cost, and yet circumvent the hurdles associated with material of biological source. However, a lack of understanding of the nature of native mucus impedes the advancement of such bio-inspired mucus models.

Early work by Larhed et al (Larhed, Artursson, and Björk, 1998), provided a fundamental overview of the composition of porcine jejunal mucus. The adaptation by Boegh et al. (Boegh et al., 2014) resulted in the development of a biosimilar mucus reflecting the properties of native porcine mucus of jejunal origin. The biosimilar mucus is a well-informed *in vitro* model that can be prepared with commonly used chemicals. It has been implemented in various experimental settings and has contributed to their improved biorelevance, by representing the barrier properties of mucus of small intestinal origin (Birch et al., 2018; Boegh et al., 2015; Falavigna et al., 2021). However, a recent study comparing mucus from various porcine GI segments reports substantial differences both in composition and structure between mucus of small and large intestinal origin (Barmpatsalou et al., 2021). These findings highlight the need for the development of an artificial mucus model based on the colonic mucus characteristics. Such a model would improve the predictive power of preclinical assessments for colonic absorption. In the present work, we report the development and validation of an artificial colonic mucus model. It was based on the characterization of porcine native colonic mucus and captured the properties of porcine proximal colonic mucus. The inter- and intra-batch variability of the artificial mucus was assessed under various storage conditions, with the aim of evaluating the potential of our model for incorporation into routine *in vitro* preclinical assessments.

2. Materials and methods

2.1. Materials

Fluorescein isothiocyanate (FITC)–diethylaminoethyl (DEAE)–dextrans (cationic), FITC– carboxymethyl (CM)–dextrans (anionic) with molecular weights of 4 and 40 kDa, and fluorescein isothiocyanate (FITC)–dextrans with molecular weights of 4, 40 and 70 kDa were purchased from Sigma–Aldrich (St. Louis, MO, USA). 2-(N-morpholino) ethanesulfonic acid (MES), polysorbate 80 (Tween 80), $CaCl_2$, $MgSO_4$, cholesterol, one lot each of Type II and III mucin from porcine stomach, and bovine serum albumin (BSA) were also obtained from Sigma Aldrich. Phosphatidylcholine (PC, 98%) was provided by Lipoid (Ludwigshafen, Germany), NaCl was purchased from Merck Chemicals (Darmstadt, Germany), and polyacrylic acid (PAA) (Carbopol 974P NF) was obtained from Lubrizol (Brussels, Belgium).

2.2. Collection of native porcine colonic mucus

The colonic mucus collection was performed as previously described (Barmpatsalou et al., 2021). Briefly, the gastrointestinal tract (GIT) of crossbreed Landrace × Large White pigs (n = 5, P01-P05), 20–22 weeks of age and 100–110 kg of body weight, was collected from a local abattoir. No ethical permit was required, as the animals were slaughtered for commercial meat production. As per the abattoir's standard procedures, the animals were fasted ≥12 h prior to slaughter with water allowed *ad libitum*.

The sample collection was initiated within 1 h after slaughter and the temperature of the tissue was monitored during collection. The first part of the large intestine (distal to the ileo-cecal valve) was opened longitudinally and submerged into ice-cold isotonic buffer (10 mM MES buffer containing 1.3 mM $CaCl_2$, 1.0 mM $MgSO_4$, and 137 mM NaCl, pH 6.5) to remove intraluminal contents. Thereafter mucus was collected with a small spatula. The sample collection was completed within 1 h and the pH was measured using a micro-electrode (Orion Sure-Flow, Thermo Fisher Scientific). Samples were aliquoted and stored at -80 ℃ until further analyses. The colonic mucus samples from P02 and P03 were used for method development purposes, and therefore colonic mucus samples from P01, P04 and P05 were included in further analyses.

2.3. Preparation of porcine artificial colonic mucus (PACM)

The preparation of PACM samples was inspired by the recently reported characterization of porcine proximal colonic mucus (Barmpatsalou et al., 2021) and was based on protocols proposed by Boegh et al. (Boegh et al., 2014). There are two types of porcine gastric mucin commercially available (Types II and III); these have undergone different purification processes. As mucins are a key component in mucus, mucin type II or type III were added to PACM (hereafter $PACM_{II}$ and $PACM_{III}$) to assess which type was best suited for the development of PACM. PACM contained 0-1.8% (w/v) PAA, 0.91% (w/v) mucin type II or mucin type III, 7.02% (w/v) BSA, 1% (v/v) lipid mixture (0.21% cholesterol and 0.12% phosphatidylcholine, mixed with Tween 80 at a 3:1 ratio). The lipid mixture was prepared by dissolving the lipids in isotonic buffer (10 mM MES with 1.3 mM $CaCl_2$, 1.0 mM $MgSO_4$, and 137 mM NaCl, pH 6.5) in the presence of Tween 80 and under intense stirring.

PAA was dissolved in a non-isotonic buffer (10 mM MES with 1.3 mM

$CaCl_2$, 1.0 mM $MgSO_4$, pH 6.5). Mucin type II or III was added to the PAA-containing solution and the resulting mixture was vigorously vortexed until all solids were dissolved. Subsequently, NaOH (5M) and BSA were added and the resulting mixture was vortexed again to dissolve all visible solids. Finally, the lipid mixture was added and the pH adjusted to 7.0 by dropwise addition of NaOH (5M). The mixture was stored overnight at 4 ℃, then placed at -80 ℃ until further analyses, unless otherwise indicated.

2.4. Water content determination

Water content of the porcine native colonic mucus was measured by transferring the samples to a laboratory-scale freeze-dryer (VirTis Sentry 2.0, SP Scientific, or a Flexi-Dry MP, FTS systems, both from CiAB, Sweden) with a condenser temperature of -80 ℃. After 48h, the samples were removed and weighed and the water content was calculated based on the weight difference of the samples before and after freeze-drying.

2.5. Zeta potential measurements

Native or artificial mucus (50 mg) was dispersed in 10 ml distilled water and stirred with a magnetic stirrer until it dissolved. An appropriate volume was transferred to an Omega cuvette and analyzed with a Litesizer 500 (Anton Paar, Austria) dynamic light scattering instrument. The measurements were conducted at 25°C, after 1 min equilibration, using the Smoluchowski approximation and Henry Factor of 1.5. The data (3-5 measurements per sample) were processed with the Kalliope software (Anton Paar, Austria).

2.6. Rheological measurements

All frozen mucus samples (native and artificial) were thawed at room temperature before the rheological measurements. An ARES-G2 strain-controlled rheometer (TA Instruments, Sollentuna, Sweden) with the Advanced Peltier System (APS) accessory for the lower plate was used. The lower geometry was a 60-mm diameter, APS quick-change flat plate from hardened chromium. A 40-mm diameter stainless steel cone plate (20μm gap, 0.98° cone angle) was used as upper geometry for all measurements except the ones performed on the native mucus samples, due to the limited available volume and the presence of μm-sized particles. Therefore, an 8-mm diameter stainless steel parallel plate (0.5 mm gap) was used as an upper geometry for the native mucus samples. Under continuous flow conditions, the apparent viscosity of the mucus samples was measured by ramping the shear rate from 0.1 to 100 s^{-1}. The viscoelastic properties of the mucus were calculated from frequency sweeps (range 0.63–20 rad/s, at 1% oscillation strain). An amplitude sweep, during which the oscillation strain was increased from 0.1 to 100% at a frequency of 1 Hz oscillation, was performed to determine the linear viscoelastic region (LVR). The 1% oscillation strain was chosen as it was within the LVR and thus ensured that the sample structure remained intact during the measurements. All measurements were performed at 37 ℃.

2.7. Cryo-scanning electron microscopy (SEM) – Image analysis

Cryo-scanning electron microscopy (cryo-SEM) analyses were performed at the Umeå Centre for Electron Microscopy (UCEM), Sweden. All samples were thawed at room temperature and one drop from each cast onto a metal holder, then vitrified in liquid nitrogen. The vitrified sample was then fractured with a cold knife and sublimated in vacuum at -90 ℃ for 30 or 60 min. Images were taken using a Carl Zeiss Merlin field-emission cryogenic scanning electron microscope, fitted with a Quorum Technologies PP3000T cryo preparation system. Imaging was performed at - 140 ℃ using an in-chamber secondary electron detector (ETD) at an accelerating voltage of 2 kV and a probe current of 50 pA. Cryo-SEM images were appropriately thresholded and converted to binary images, and the pores were identified and characterized (in terms of size and shape) by the ImageJ software (Version 1.52a, NIH, USA). Feret's minimum diameter, i.e. the shortest distance between any two parallel tangents of a pore, was used as the pore size descriptor. The Aspect Ratio (AR), the ratio of Feret's max (F_{max}) diameter to Feret's min (F_{min}) diameter (Eq. (1)), was used as the pore shape descriptor.

$$AR = \frac{Fmax}{Fmin} \tag{1}$$

2.8. Fluorescence recovery after photobleaching (FRAP) and diffusivity calculations

FRAP experiments were performed to elucidate the impact of charge and molecular weight on diffusion. FITC–dextrans were used in a range of charges and molecular weights: 4 and 40 kDa for both cationic and anionic FITC–dextran molecules, and 4, 40 and 70 kDa for the non-ionic ones. The diffusion of the FITC-dextrans was assessed in the native and artificial mucus, and in a PAA mixture. FITC-dextrans were dissolved in Hanks' Balanced Salt Solution (HBSS) buffer, pH at 7.4 (0.625 mg/ml) and 20 μL of the solution was transferred to 80 mg of mucus sample. The sample was first vortexed and then mechanically mixed using a pipette tip to ensure homogenous distribution of the fluorophore in the hydrogels.

To ensure consistent sample thickness across all experiments, each mucus sample was pipetted between two glass coverslips (one on each end) which were placed onto a microscope slide, as previously illustrated (Peng et al., 2021). The mounting of the mucus sample was finalized by placing a coverslip on top of the mucus sample, resulting in a fixed sample thickness of 100 μm. Thereafter, the microscope slide was promptly imaged, to avoid drying of the gel and underestimation of the diffusivity values.

FRAP measurements were performed using a Zeiss CLSM 780 and the data were collected with the ZEN Black software (Carl Zeiss GmbH, Jena, Germany). All bleaching experiments were performed with the 488-nm line of an Argon laser at 100% power. A 20 × objective lens (CFI Plan Apochromat) with a numerical aperture (NA) of 0.8 was used. Each experiment was initiated by adjusting the detector gain to an appropriate value to ensure no pixels were saturated. Homogenous distribution of the fluorophore in the gel was confirmed by imaging various sample areas. In the initial studies, no fluorescence was observed in mucus samples in the absence of FITC dextrans (Fig. S1). Two circular regions of interest (ROI) with a 16-μm radius each were selected. The two ROIs were then included in a rectangular frame, and only pixels in the rectangle were imaged, to increase the rate of data acquisition. After scanning three images, one ROI was bleached, while the other ROI was not bleached and served as a reference to monitor potential photofading. A time series of 150 images was immediately taken at 2.2% laser transmission in 1.5-s intervals, to monitor fluorescence recovery in the bleached ROI. All measurements (n≥ 3) were performed at room temperature.

Diffusivity values were calculated as previously described (Brandl et al., 2010). The fluorescence intensities of the bleached and reference ROIs were initially normalized to the pre-bleach intensity (fluorescence intensity inside the ROI as recorded in the last caption right before the bleaching event). A least-squares fit was performed on the recovery curve (Eq. (2)) in R (code available upon request) to determine the characteristic diffusion time τ_D.

$$F(t) = k \cdot e^{-\frac{\tau D}{2t}} \left[I_o \left(\frac{\tau D}{2t} \right) + \mathrm{I}_1 \left(\frac{\tau D}{2t} \right) \right] \tag{2}$$

where I_0 and I_1 are the zero and first-order modified Bessel functions of the first kind, respectively, k corresponds to the mobile fraction, and t is time (s). The diffusivity values were obtained by solving $D = w^2/\tau_D$, where w is the radius of the bleached ROI (16 μm).

2.9. Impact of production and storage conditions

To explore inter-batch variability, three batches of PACM were prepared independently under the same conditions. As described in the PACM preparation protocol, the three PACM batches were stored at 4 ℃ overnight. The next day, each batch was divided into three equal portions and each portion thereof ("fresh", "frozen" and "freeze-dried") was stored as follows. The portion of each batch corresponding to the "fresh" condition, underwent rheological assessment and diffusivity measurements on the same day. The remaining sample volume was then stored at -80 ℃ prior to Cryo-SEM imaging. The remaining two portions were stored at -20 ℃ ("frozen"), or -80 ℃ ("freeze-dried"). On the day of the rheological and diffusivity measurements, the portions of each batch stored at -20 ℃ were thawed at room temperature. After these measurements, the remaining sample volume was stored at -80 ℃ for Cryo-SEM analysis. The portions representing the "freeze-dried" condition were stored at -80 ℃ and transferred to a laboratory-scale freeze dryer with a condenser temperature of -80 ℃. After 48h, the samples were reconstituted to their initial volume with MilliQ water and left to equilibrate for 10 minutes on a laboratory bench. Thereafter, rheological and diffusivity measurements were performed, both on the same day. At the end of the measurements, the remaining sample volume was stored at -80 ℃ for later Cryo-SEM imaging.

2.10. Data Visualization-Statistics

GraphPad Prism (GraphPad Software, CA, USA) was used for data visualization and statistical analyses. A one-way ANOVA, followed by Holm-Sidak's multiple comparisons test, was used to evaluate differences between more than two groups. P values less than 0.05 were considered statistically significant.

3. Results

3.1. Rheology

3.1.1. Inter- and intra-animal variability in the rheology of porcine native colonic mucus

All colonic mucus samples had a gel-like texture upon visual observation and exhibited viscoelastic properties and shear thinning behavior. Apparent viscosity values decreased at increasing shearing rates (Fig. 1A).

The inter- and intra-animal variability of the shear-rate dependent rheological profiles are depicted in Fig. 1A, for the colonic mucus collected from three pigs (P01, P04 and P05). Due to limited sample, only one pig (P04) was selected to undergo the intra-animal variability assessment. The inter-animal variability in apparent viscosity at shear rate 0.91 s^{-1} was 6-fold (difference between the maximum and minimum values), while the intra-animal variability was 2-fold.

The viscoelastic properties of the native porcine colonic mucus were assessed and the storage modulus (G') and loss modulus (G'') were measured under dynamic oscillatory shear conditions. In all cases, the storage modulus values were higher than the loss modulus ones throughout the range of the examined angular frequencies, indicating predominantly elastic behavior (data of loss moduli are not shown for clarity). The storage modulus profiles of porcine colonic mucus are displayed in Fig. 1B, and show they were independent of the angular frequency. The inter- and intra-animal variability (at angular frequency 1 rad/s) was 10-fold and 3-fold, respectively.

3.1.2. Rheological validation of porcine artificial colonic mucus (PACM)

PACM was formulated based on the composition of native porcine colonic mucus (Barmpatsalou et al., 2021). Initial preparations of $PACM_{II}$ and $PACM_{III}$ were not gel-like. Therefore, polyacrylic acid (PAA) was added to increase the apparent viscosity and the cross-linking (Boegh et al., 2014). Both PACM samples were prepared and stored at -80 ℃ until the rheological analysis, to replicate the storage conditions in a previous rheological study (Barmpatsalou et al., 2021). Fig. 2A and B display the apparent viscosity and storage modulus profiles of $PACM_{II}$ samples with increasing PAA concentrations. The rheological properties of $PACM_{II}$ and $PACM_{III}$ that contained 1.5% (w/v) PAA were in agreement with those of native porcine colonic mucus reported here and in previous investigations (Barmpatsalou et al., 2021); see Fig. 2C and D. Thus, the $PACM_{II}$ and $PACM_{III}$ samples with 1.5% (w/v) PAA were selected as the most representative of the native mucus secretion and used in further analyses.

3.1.3. Impact of storage conditions on the rheological properties of $PACM_{II}$

The impact of the three storage conditions (fresh, frozen at -20 ℃, and freeze-dried/reconstituted with MilliQ water) on the rheological properties of $PACM_{II}$ under continuous rotation and oscillatory shear conditions was assessed (Figs. 3A, B and S2). There were no significant differences in apparent viscosity profiles (at 1 s^{-1}) or storage modulus values (at 1 rad/s) values for the three conditions. In the case of multiple measurements per batch (for the intra-batch variability assessment), the average value was included in the calculations.

3.1.4. Inter- and intra-batch variability in the rheological properties of $PACM_{II}$

The inter- and intra-batch variability of the rheological properties of the $PACM_{II}$ batches under the three storage conditions was assessed and is shown in Figs. 3A, B and S3. The inter-batch variability in apparent viscosity values at a shear rate of 1 s^{-1} was 2-fold for the frozen and freeze-dried $PACM_{II}$ and 3-fold for the fresh ones. The intra-batch

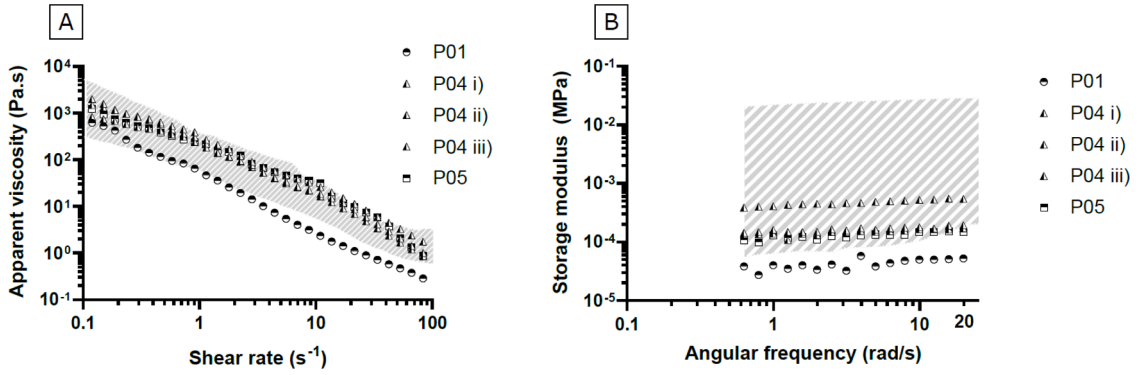

Fig. 1. Inter- and intra-animal variability assessment of the rheological properties of porcine native colonic mucus for three pigs (P01, P04, and P05). Apparent viscosity curves of porcine proximal colonic mucus samples as a function of shear rate (A), Storage modulus profiles of porcine proximal colonic mucus samples as a function of angular frequency (B). Shaded area represents the range of data from a previous investigation (Barmpatsalou et al., 2021). i), ii) and iii) represent multiple independent measurements of colonic mucus samples from pig P04.

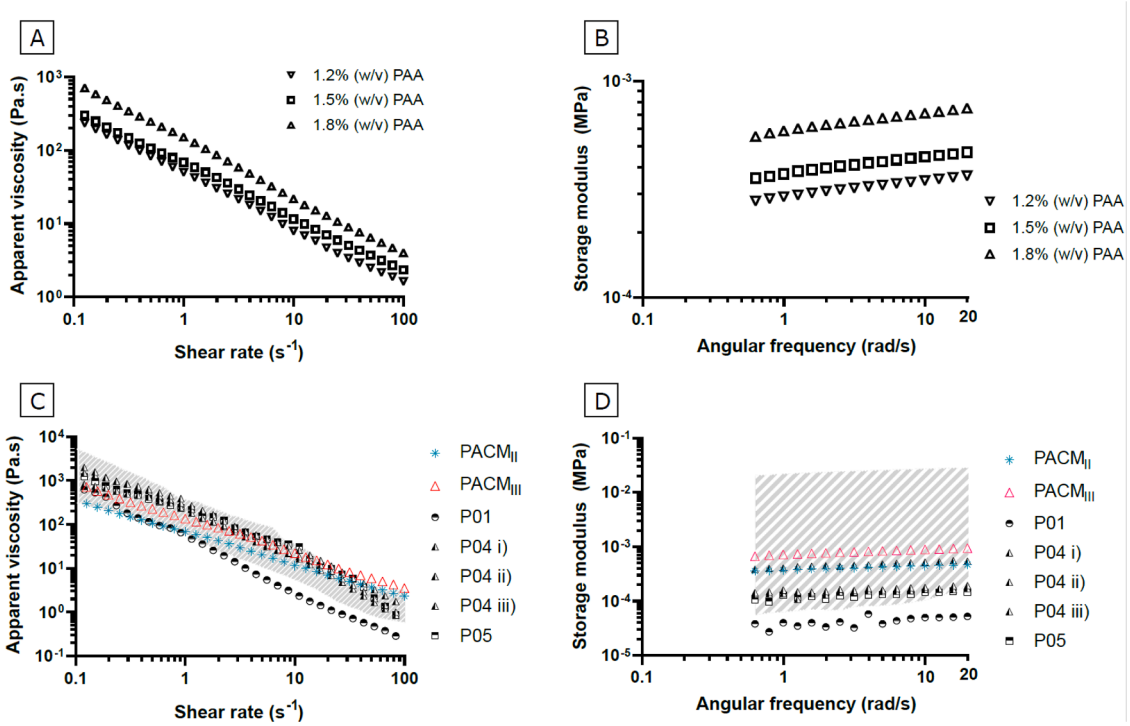

Fig. 2. Rheological profiling of PACM: Effect of increasing amounts of PAA in the apparent viscosity (A) and storage modulus (B) of $PACM_{II}$ samples. Reverse triangles, squares and triangles represent 1.2%, 1.5% and 1.8% (w/v) PAA additions to the samples. Comparison of PACM and native porcine colonic mucus in terms of apparent viscosity (C) and storage modulus (D) values. The shaded area represents the range of data from a previous investigation (Barmpatsalou et al., 2021). $PACM_{II}$, blue stars; $PACM_{III}$, red triangles. Native colonic mucus values are from three pigs (P01, P04, and P05), represented in black circles, triangles, and squares, respectively. i), ii) and iii) represent multiple independent measurements of colonic mucus samples from pig P04.

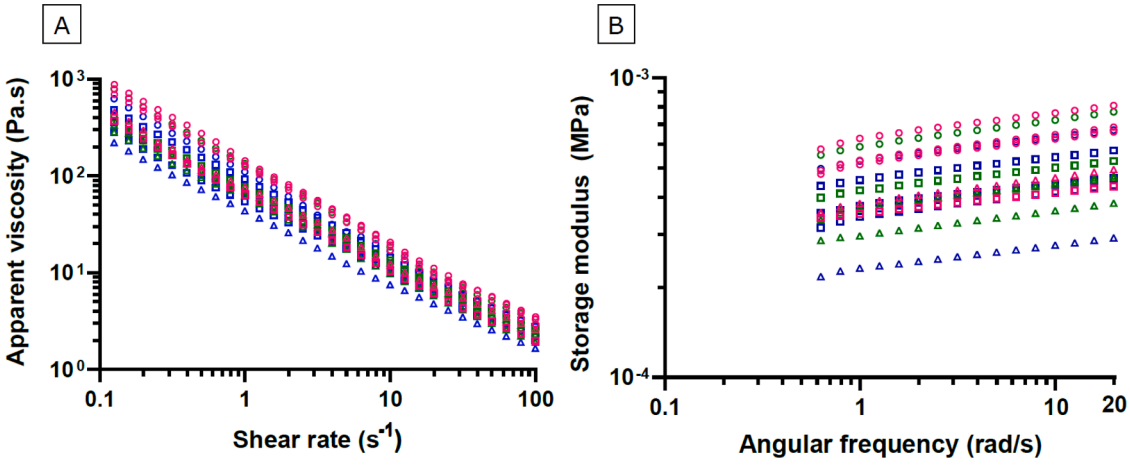

Fig. 3. Impact of storage conditions and assessment of inter- and intra- batch variability on the rheological properties of $PACM_{II}$: Apparent viscosity (A) and storage modulus (B) profiles. Triangles, circles, and squares represent batches 1, 2, and 3, respectively. Samples stored as fresh, frozen at -20 ℃, and freeze-dried are noted with blue, green, and pink colors, respectively. For each storage condition, one batch was selected to undergo the intra-batch variability assessment and thus three measurements were recorded for these.

variability was 2-fold for the fresh $PACM_{II}$ batches and negligible for the frozen and freeze-dried ones. The storage modulus profiles of the batches are outlined in Figs. 3B and S3. The inter-batch variability at 1 rad/s frequency was 2-fold for all conditions. Variability was negligible for the intra-batch samples, irrespective of storage condition.

3.2. *CryoSEM - image analysis*

3.2.1. *Validation of porcine artificial colonic mucus based on gel network microarchitecture*

The gel network microarchitecture of $PACM_{II}$ and $PACM_{II}$ was visualized with Cryo-SEM, under the same microscopy conditions used to characterize the microarchitecture of native porcine colonic mucus in a previous study (Barmpatsalou et al., 2021).

The CryoSEM micrographs showed that neither of the initial $PACM_{II}$ and $PACM_{II}$ samples displayed gel-like characteristics in the absence of

PAA; rather, they formed "loose" structures (Fig. 4A and B). With the addition of 1.5% (w/v) PAA, the $PACM_{II}$ and $PACM_{II}$ samples adapted a "honeycomb" structure (Fig. 4C and D, respectively), resembling that of the native porcine colonic mucus (Fig. 4E). Both $PACM_{II}$ and $PACM_{III}$ had a high degree of homogeneity, as seen in the low-magnification micrographs (Fig. 4F and G).

3.2.2. Impact of storage conditions and inter-batch variability on the gel network microarchitecture of $PACM_{II}$. The effect of storage conditions (fresh, frozen at -20 ℃ and freeze-dried/reconstituted with MilliQ water) on the network microarchitecture was also assessed with Cryo-SEM (Fig. 5A-I). No significant differences in pore size or shape were found for any of the storage conditions or batches (Fig. 5J and K) and all mucus batches were homogeneous. The mean Feret's minimum diameter values ranged from 4.6-5.8, 3.4-4.4 and 3.7-4.3 for batches 1, 2 and 3, respectively, for all three storage conditions. The pore shape was similar for the three storage conditions, with mean AR values ranging from 1.7-2, 1.6-1.9 and 1.6-1.8 for batches 1, 2 and 3, respectively, in each condition.

The inter-batch variability of the pore network was also analyzed by Cryo-SEM, Fig. 5J (size) and 5K (shape). The mean Feret's minimum diameter was similar across the three storage conditions, ranging from 1.3-fold for the fresh and freeze-dried $PACM_{II}$ and 1.4-fold for the frozen one. The pore shape was also similar in the three batches, with negligible inter-batch variability (1.2-fold for fresh $PACM_{II}$ and 1.1 for the frozen and freeze-dried ones).

3.3. Diffusivity measurements

3.3.1. Diffusion of FITC dextrans in native porcine colonic mucus

The diffusion of FITC dextrans in native porcine colonic mucus was tracked by FRAP. Fig. 6A provides an overview of the diffusivity values of the 4K molecular weight FITC-dextrans (neutral, anionic, and cationic) in native colonic mucus samples from three pigs (P01, P04, and P05). A trend was observed towards decreased diffusivity values of cationic FITC- dextran compared to the anionic and neutral ones.

For pigs P01 and P05, there was no significant difference between the diffusivity values of the neutral and anionic 4K FITC-dextrans. However, these values were significantly higher than those of the cationic FITC-dextran (Fig. 6B and D). For pig P04, the diffusivity values of the anionic and cationic 4K FITC-dextrans were significantly different from each other and both were significantly lower than that of the neutral 4K FITC dextran (Fig. 6C).

Fig. 6E presents the diffusivity values of the neutral and anionic 40K FITC-dextrans from the same three pigs. No significant differences between the diffusivity values were observed. The diffusion of the cationic 40K FITC-dextran was also assessed. However, recovery of the fluorescence was very slow, and thus diffusivity values could not be calculated. Representative confocal images of the fluorescence recovery within colonic mucus from pig P04 at various time points are presented in Fig. 6Fi-iii. It is evident that the cationic 40K FITC-dextran was non-homogenously distributed in the mucus sample. Instead, it was bound to specific sites of the gel network, despite the thorough mixing. Fig. 6G depicts the diffusivity values of FITC-dextrans of various molecular sizes

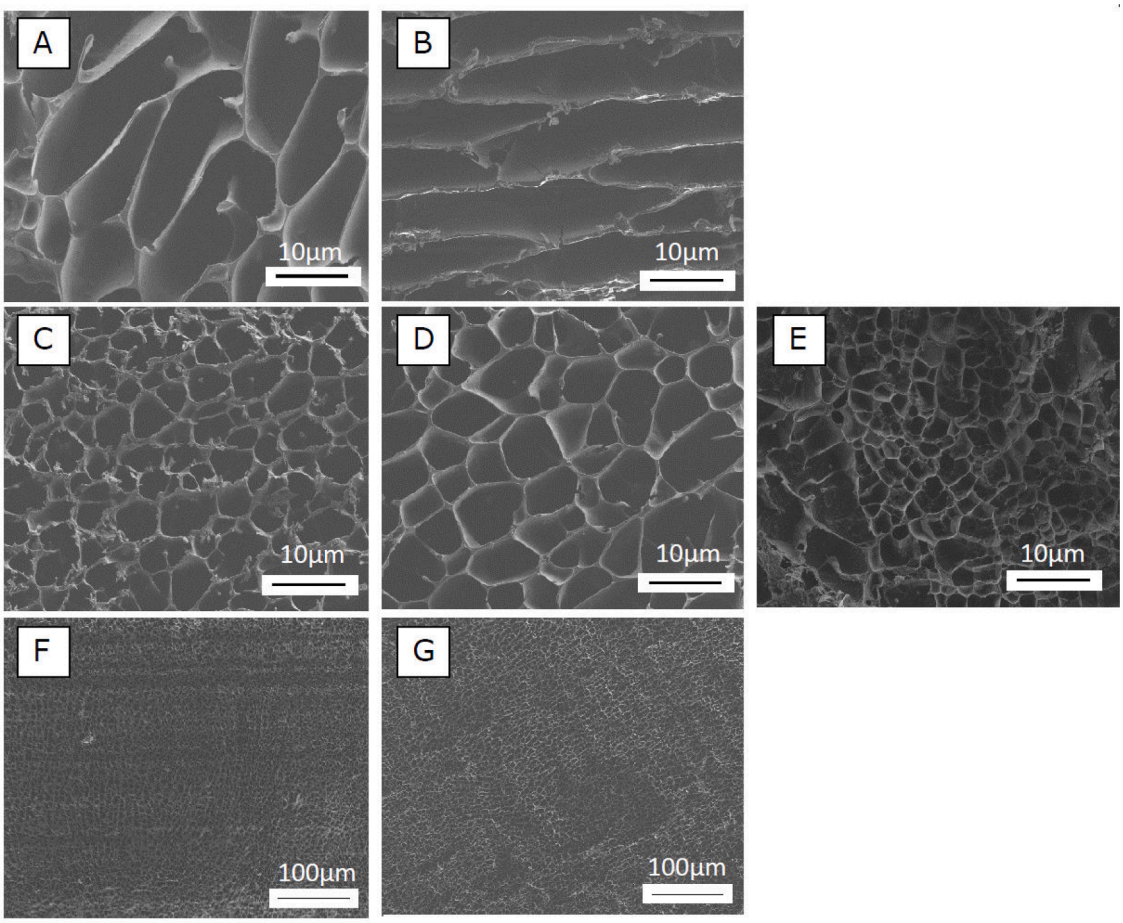

Fig. 4. Structural validation of $PACM_{II}$ and $PACM_{III}$: Representative cryo-scanning electron micrographs of $PACM_{II}$ samples without PAA (A), $PACM_{III}$ samples without PAA (B), $PACM_{II}$ samples with 1.5% (w/v) PAA (C), $PACM_{III}$ samples with 1.5% (w/v) PAA (D), native porcine colonic mucus (E), all at 5000 × magnification. Scale bars (A-E): 10 µm. Representative cryo-scanning electron micrographs of $PACM_{II}$ (F) and $PACM_{III}$ (G), both with 1.5% (w/v) PAA at 500 × magnification. Scale bars: 100 µm (F-G).

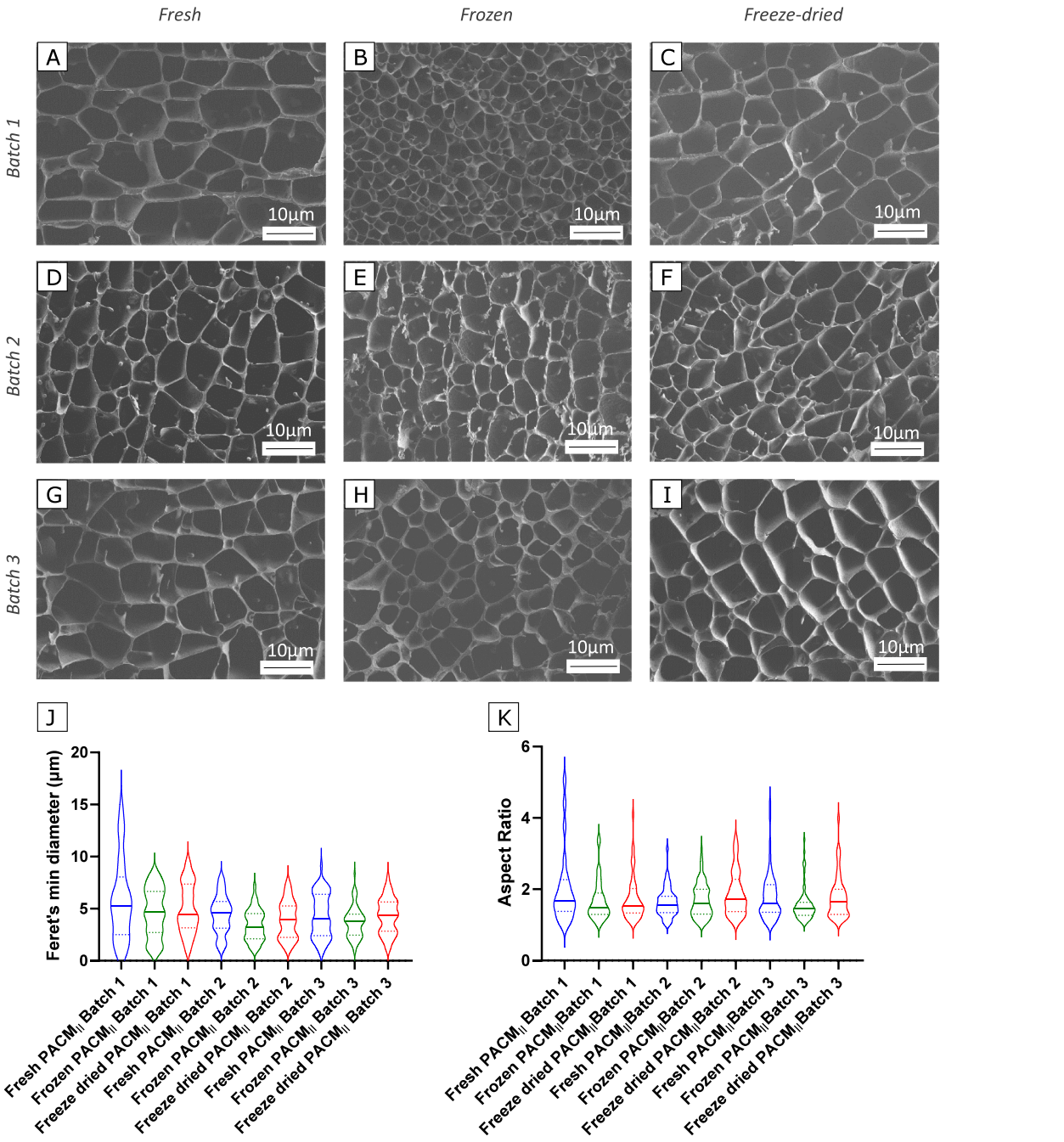

Fig. 5. Impact of storage conditions and inter-batch variability on the gel network microarchitecture of $PACM_{II}$: Representative cryo-scanning electron micrographs of three batches of $PACM_{II}$ under three storage conditions. 5000 × magnification (5A-5I). Scale bars: 10 µm. Comparison of mucus pores from three $PACM_{II}$ batches stored under three conditions (fresh, frozen, freeze-dried). Violin plots of Feret's minimum diameter (J) and Aspect Ratio (K) distribution. Dotted lines represent the 25% and 75% percentiles, while bold line represent the median.

(4K, 40K, and 70K). In all three animals, the diffusivity values of 4K FITC-dextran were significantly higher compared to 40K and 70K, as shown in Fig. 6H-J. No significant differences between the diffusivity values of 40K and 70K FITC-dextrans were identified.

3.3.2. Validation of porcine artificial colonic mucus (PACM) based on diffusion of FITC dextrans. The $PACM_{II}$ and $PACM_{III}$ samples containing 1.5% (w/v) PAA mimicked the rheological properties of the native porcine colonic mucus. These were therefore selected for validation against the native mucus in terms of the diffusion profiles of the different charge and size FITC-dextrans. Pure PAA aqueous gel containing PAA in equal amounts to $PACM_{II}$ and $PACM_{III}$ was also investigated to assess whether PAA alone could adequately capture the complex physico-chemical interactions and size exclusion properties of native colonic mucus. If this were to be the case, the PAA mixture could replace the artificial mucus samples.

Fig. 7A and B depict the diffusivity values of the FITC-dextrans of various charges and sizes in $PACM_{II}$, $PACM_{III}$, PAA gel, and the pooled data of native porcine colonic mucus origin. In all cases except for the cationic 4K FITC-dextran, the diffusivity values from $PACM_{II}$ and $PACM_{III}$ were not significantly different from the pooled values from native porcine colonic mucus origin. The diffusivity values of neutral and anionic 4K FITC-dextrans obtained from the PAA gel were significantly higher compared to the respective values from the pooled values from

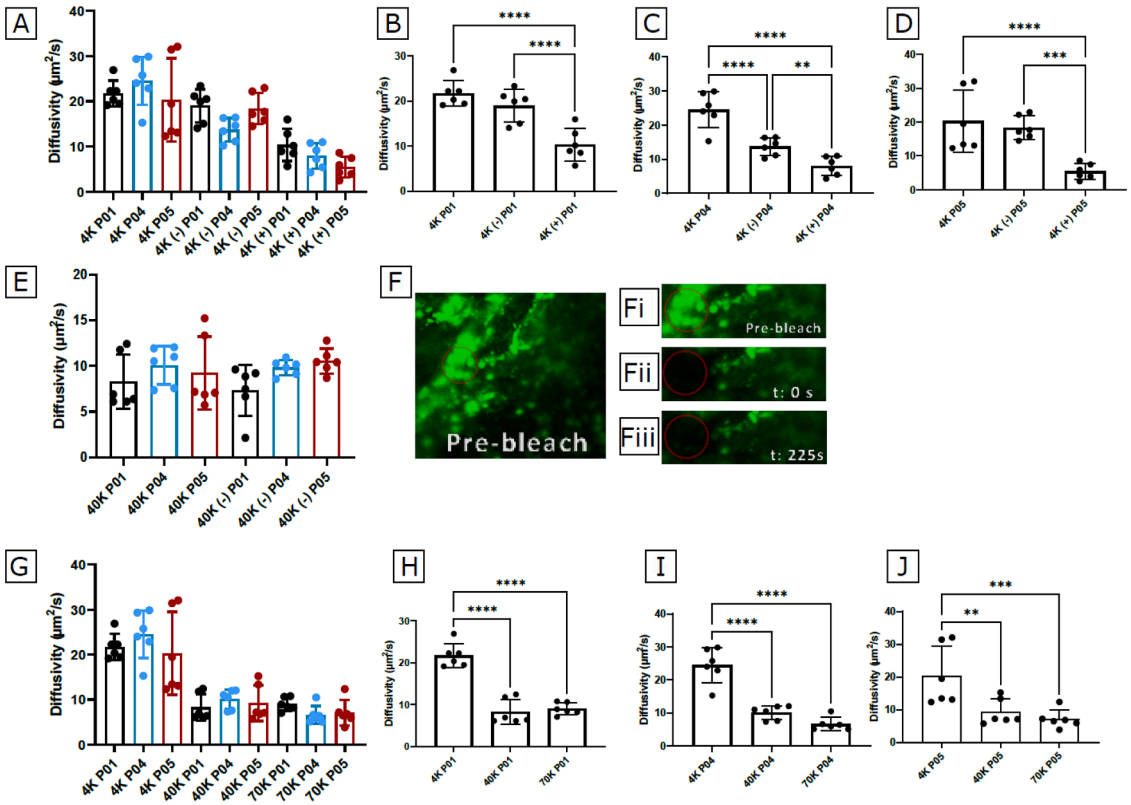

Fig. 6. Comparison of FITC-dextran diffusivity values in native porcine colonic mucus. Diffusivity values of neutral, anionic (-) and cationic (+) 4K FITC-dextrans in native colonic mucus from three pigs (P01, P04 and P05) (A), Individual profiles and statistical analysis of diffusivity values from P01 (B), P04 (C) and P05 (D). Diffusivity values for the neutral and anionic (-) 40K dextrans in native porcine colonic mucus from the same three pigs (E). Confocal images of native colonic mucus of pig P04 during a FRAP experiment with the cationic (+) 40K FITC-dextran (F), including pre-bleach caption (Fi). Captions were taken immediately after the photobleaching event (Fii) and at t: 225 s (Fiii). Diffusivity values of the 4K, 40K, and 70K FITC-dextrans (G) from three pigs (P01, P04, and P05) and respective individual profiles and statistical analysis for P01 (H), P04 (I) and P05 (J); n=3-6. Filled circles represent individual measurements. Bars: Mean±SD.

native porcine colonic mucus origin, while the diffusivity values of cationic 4K FITC-dextran in PAA and PACM were similar to each other and significantly lower compared to the pooled values from native porcine colonic mucus origin. There was no significant difference in the diffusivity values between the PAA gel and the pooled values from native porcine colonic mucus origin of the FITC-dextrans with higher molecular weight that were assessed (neutral and anionic 40K and neutral 70K). A good correlation between the diffusivity values of FITC-dextrans in $PACM_{II}$ and porcine native colonic mucus was established (R^2: 0.99); see Fig. 7C.

3.3.3. Impact of storage conditions on the diffusion of FITC-dextrans in $PACM_{II}$. The impact of storage conditions on the diffusivity of FITC-dextrans was investigated by FRAP. Fig. 8A and B provide an overview of the diffusivity values of FITC-dextrans of various charge and size properties obtained for measurements in $PACM_{II}$ stored in various conditions. The values were within the variability observed for the diffusion of FITC-dextrans in native porcine colonic mucus (shaded area), except cationic 4K FITC-dextran, for which diffusivity values were lower in the artificial mucus. No trend in the diffusivity values could be observed for any of the storage conditions.

4. Discussion

4.1. Key properties of porcine native colonic mucus

4.1.1. Inter- and intra-animal variability in the rheology of the porcine native colonic mucus

All colonic mucus samples from the three pigs showed pseudoplastic behavior, with the apparent viscosity values decreasing with increasing shear rates (i.e., shear-thinning characteristics). This was in agreement with data from a previous investigation (illustrated as a gray area in Fig. 1A.), where the mucus collection and the rheological assessment were performed using the same protocols as the present study, and therefore any variation in the results would be attributed to variations in the animal material (natural variation) rather than variations between labs or protocols. The inter-animal variability was 6-fold, again in accordance with previously reported values (8-fold, (Barmpatsalou et al., 2021), <3-fold (Dubbelboer et al., 2022)), and lower than the inter-animal variability for small intestinal mucus (14-fold (Curt and Pringle, 1969), 18-fold (Barmpatsalou et al., 2021), and 25-fold (Boegh et al., 2014)). Colonic mucus from pigs P04 and P05 had similar apparent viscosity values throughout the range of examined shear rates. Pig P01 had lower apparent viscosity values than P04 and P05. It is unlikely that this difference can be attributed solely to water content or pH properties, as there was no correlation between these physiological properties and the apparent viscosity values for the three pigs (Table S1). This suggests that the apparent viscosity results from synergistic effects of various factors. The relatively limited inter-animal variability might be related to the well-controlled environment in which pigs are farmed. Efforts towards the production of standardized meat for commercial consumption have been intensified (Agostini et al., 2015), resulting in the adaptation of standardized routines and procedures in animal farming. Therefore, farmed animals have access to the same type of food and are kept in similar environments, aspects that contribute to similar characteristics. Additionally, as the inner layer of the colonic mucus must withstand high shear rates so that it can protect the colonic epithelium, it is crucial to have a continuous mucus layer with similar rheological characteristics for the homeostasis of the GIT, as

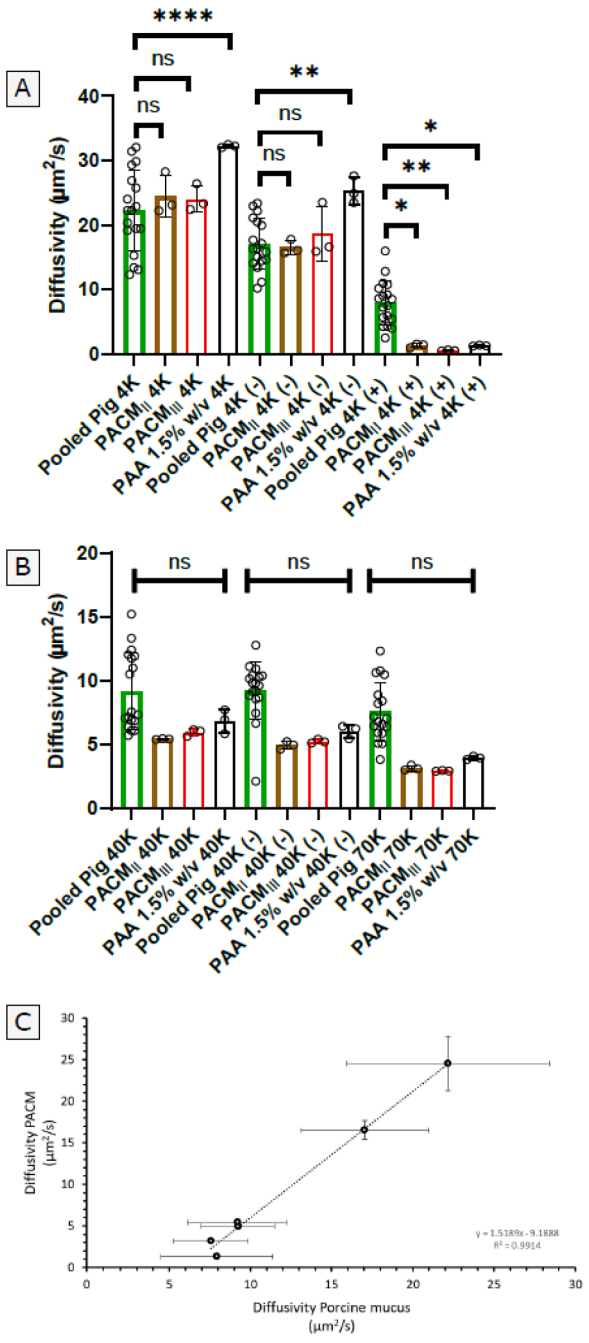

Fig. 7. Comparison of diffusivity values of FITC-dextrans in native porcine colonic mucus from three pigs (P01, P04, and P05), in $PACM_{II}$, $PACM_{III,}$ and PAA 1.5% (w/v) gel: 4K (A), 40K and 70K molecular weights (B). Open circles represent individual measurements. n: 3-6, Bars: Mean±SD. Correlation between average diffusivity values of various FITC-dextrans in $PACM_{II}$ and porcine native colonic mucus (Mean±SD) (C).

reflected in the limited intra-animal variability (2-fold).

The rheological properties of mucus play a crucial role in regulating the transport of nutrients, drugs, and particles (Bansil and Turner, 2006) through the epithelium. Significantly reduced viscosity is associated with bacterial adhesion in gastric mucus (Chen et al., 2010), while increased viscosity can be related to mucus accumulation and eventually GIT obstruction (Chen et al., 2010; Meldrum et al., 2018). As the rheological profile of mucus is associated with the GIT homeostasis, the variability between animals is within a range that allows proper mucus functionality.

The storage moduli (*G'*) of colonic mucus from pigs P04 and P05 were in line with previously reported data (Barmpatsalou et al., 2021; Sellers et al., 1991), as shown in Fig. 1B. The dominance of *G'* is a characteristic of cross-linked polymers which relates to solid-like properties (Ruiz-Pulido and Medina, 2021; Huck et al., 2019). Colonic mucus of these two pigs showed similar storage modulus values and thus similar extent of crosslinking. In contrast, colonic mucus from pig P01 had less cross-linking, as represented by the lower *G'* values, throughout the range of the angular frequency values. The mucus from pig P01 had a higher pH-value than mucus from pigs P04 and P05 (7.3 vs 7.1 and 7.0, respectively). However, this is unlikely to be the reason for the difference in their rheological profiles, as significant conformational changes in the mucins require larger pH variations (such as pH 2 and 4 vs. pH 6) (Ruiz-Pulido and Medina, 2021).

Inter-animal variability was 10-fold, which was lower compared to that previously reported for small intestinal mucus (15-fold (Boegh et al., 2014)). This observation shows the importance of the mucus rheology for creating a barrier that protects the epithelium from the harsh intracolonic environment and bacterial load (Johansson et al., 2008). The intra-animal variability was 3-fold, similar to that observed for porcine small intestinal mucus (2-fold (Boegh et al., 2014)). The storage modulus values from all mucus samples showed frequency independence, suggesting gel characteristics for all mucus samples.

Overall, inter-animal variability was higher for the storage modulus than for the apparent viscosity. Apparently, inter-animal variation is greater for the viscoelastic properties of the mucus samples than for flow resistance. Similar observations have been reported for colonic mucus in possums (Lim et al., 2013).

4.1.2. Diffusion of FITC-dextrans in porcine native colonic mucus. The diffusion of FITC-dextrans in porcine native colonic mucus was used to assess the impact of charge and size on molecular diffusion. As seen in Fig. 6A-D, the negatively charged 4K FITC-dextran tended to have slightly decreased diffusivity values, compared to the neutral one. This may be related to repulsive forces between the anion and the negatively charged sialic acid and sulfate sugar residues on the mucin glycoproteins (Desai and Vadgama, 1991; Araújo et al., 2018; Fröhlich and Roblegg, 2014) . However, the difference between diffusivity values for the neutral and negatively charged FITC-dextrans was only significant in colonic mucus from a single pig. In contrast, the positively charged 4K FITC-dextran resulted in a dramatic decrease in diffusivity values for all three pigs, as shown in Fig. 6A-D. Other studies also highlight the limited diffusion of positively charged molecules in porcine gastric mucus (Desai and Vadgama, 1991) and nanoparticles in porcine jejunal mucus (Crater and Carrier, 2010). Such phenomena can be attributed to electrostatic interactions between the diffusing cation and the negatively charged mucin domains (Cobarrubia et al., 2021; Griffiths et al., 2015).

The negatively charged and neutral 40K FITC-dextrans had comparable diffusivity values (Fig. 6E). This might be related to the higher molecular weight. It dominates diffusion behavior, contributing to decreased mobility, whereas repulsive physicochemical interactions have limited contribution to the diffusion profile. Nevertheless, the positive charge in the high molecular-weight FITC-dextran resulted in complete immobilization and physicochemical entrapment within the porcine colonic mucus network (Fig. 6F). Substantial differences have been previously reported between the diffusion of anionic and cationic synthetic peptides of equal molecular weight in porcine gastric mucus (Li et al., 2013) and between the diffusion of anionic and cationic 40K FITC-dextran in a mucin solution (Peng et al., 2021). This suggests that permeation of high molecular-weight cations is highly restricted through porcine colonic mucus.

Fig. 6G-J illustrate the effect of molecular weight on the diffusion of FITC-dextrans through porcine colonic mucus. Diffusivity of the FITC-dextrans decreased with increase in molecular weight. Higher molecular weight might be associated with decreased mobility and increased

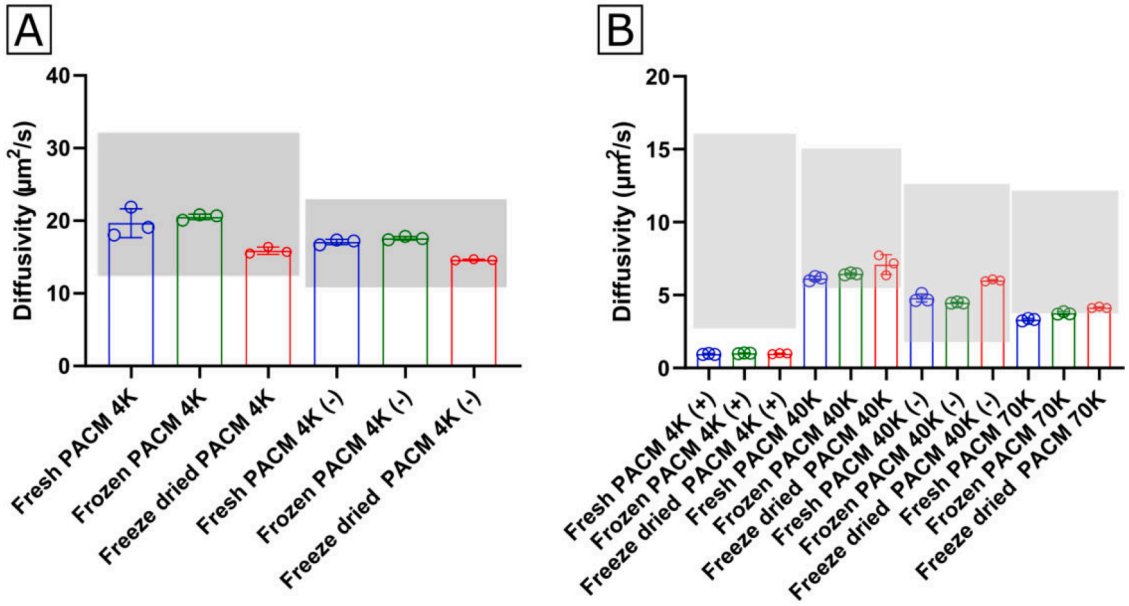

Fig. 8. Impact of storage conditions on the diffusion of FITC dextrans in $PACM_{II}$: Diffusivity values of FITC dextrans in $PACM_{II}$ samples stored under various storage conditions. Fresh, frozen and freeze-dried are depicted in blue, green and red, respectively. Neutral and anionic 4K (A), cationic 4K, 40K and 70K molecular weights (B). The shaded area represents the range of data obtained from porcine native colonic mucus in the present study. Open circles represent individual measurements, Bars: Mean±SD.

likelihood of physicochemical interactions. In the present study, 40K and 70K FITC-dextrans exhibited lower diffusivity values in colonic mucus than 4K FITC-dextrans, but they were not completely immobilized. Similar observations are reported for the diffusion of macromolecules (molecular weight range 126-186,000 Daltons) in porcine gastric mucus (Desai, Mutlu, and Vadgama, 1992) and peptides (molecular weight range 3.4-66,000 Daltons) in porcine intestinal mucus (Bernkop-Schnürch and Fragner, 1996). The authors observed consistent retardation of solute flux in the mucus with increasing molecular weight, although no absolute molecular weight cut-off for the phenomenon. A recent study of FITC-dextran (4K, 40K, and 150K) diffusion in porcine jejunal mucus also reports decreasing apparent permeability values with increasing molecular weight (Støvring Mortensen et al., 2022). The decrease in diffusivity values is not proportional to the increase in molecular weight, as shown in studies on porcine gastric mucus (Desai, Mutlu, and Vadgama, 1992), porcine jejunal mucus (Støvring Mortensen et al., 2022), and human cystic fibrosis sputum (Braeckmans et al., 2003). Thus, for molecules with molecular weights above the cut-off of the mucus mesh, diffusion is substantially delayed.

4.2. Development and validation of porcine artificial colonic mucus (PACM)

The use of pigs in preclinical assessments has gained substantial interest lately (Bode et al., 2010; Colleton et al., 2016), largely due to the similarities in gastrointestinal characteristics between pigs and humans (Swindle et al., 2012). Both humans and pigs are omnivorous species (Patterson, Lei, and Miller, 2008), sharing similar digestive features and colonic microbiome (Rowan et al., 1994), and pigs have demonstrated their potential to predict most ADMET endpoints (van der Laan et al., 2010). These similarities in gastrointestinal physiology have been translated in good correlation (r^2=0.52) between the bioavailability of compounds administered in pigs and humans (Henze et al., 2019).

The labor-intensive and animal-dependent mucus collection process catalyzed the quest for *in vitro* mucus models that mimic the native secretions but can be quickly and affordably prepared in a laboratory animal-free setting. The characterization of porcine jejunal mucus (Larhed et al., 1997) shed light on the jejunal mucus composition. Further rheological measurements by Boegh et al. contributed to the development of an artificial mucus model reflecting the porcine jejunal mucus (Boegh et al., 2014). However, the composition and structural profiles differ for porcine jejunal and colonic mucus (Barmpatsalou et al., 2021), and the need for an *in vitro* mucus model reflecting the colonic mucus emerged. Early studies showed that porcine mucin isolated, purified and reconstituted into mucus had rheological properties similar to native porcine colonic mucus (Sellers et al., 1991). However, the mucin was isolated from native mucus and thus, the preparation involved the mucus collection and processing step, limiting the flexibility of this model that was still dependent on animal sources. Our goal was to develop a model with an easy preparation protocol using commonly available laboratory chemicals. The development of the artificial colonic mucus was inspired by the protocols for the preparation of porcine artificial jejunal mucus (Larhed, Artursson, and Björk, 1998; Boegh et al., 2014). The quantities of the components were adjusted to reflect the composition of native porcine proximal colonic mucus (Barmpatsalou et al., 2021), as in the upper large intestinal tract there is higher potential for drug absorption compared to the lower large intestinal segments, where the intraluminal contents have been solidified.

4.2.1. Rheological properties and gel network microarchitecture of porcine artificial colonic mucus (PACM)

The development of PACM was initiated by preparing a mixture of the mucus components. This resulted in a liquid-like sample, as previously observed (Boegh et al., 2014), and revealed a limited capacity of the commercially available mucins to form a complex gel network. That was observed for both $PACM_{II}$ and $PACM_{III}$. Mucin is known to be a key functional contributor to the gel properties of mucus, as the non-covalent bonds of the mucins are associated with the rheological properties of the mucus (Madsen, Eberth, and Smart, 1998). However, commercially available mucins have compromised amounts of glycans due to the purification process they undergo (Marczynski et al., 2021). The loss of functional groups results in limited gelling ability of the commercially available mucins (Marczynski et al., 2021), something extensively described in the literature (Kocevar-Nared, Kristl, and Smid-Korbar, 1997; Huck et al., 2019; Røn et al., 2017) and which can explain the liquid character of our samples.

PAA is known to be a highly efficient thickener that cross-links heavily upon dispersion in water. In the presence of a base, the polymer backbone is ionized and the presence of negative charges results in electrostatic repulsion forces further extending the polymer chains (Kim et al., 2003). Cryo-SEM images (Kim et al., 2003) revealed that the resulting network is comparable to native mucus and could contribute to the shear thinning and solid-like properties of the porcine artificial colonic mucus. Indeed, it has been shown that PAA is capable of associating with mucus through mucoadhesion (Riley et al., 2001), by the interpenetration of the polymeric chains into the mucus glycoprotein chains. This results in physical entanglement and functional group interactions (Ruiz-Pulido and Medina, 2021).

The gradual addition of PAA resulted in increased apparent viscosity and storage modulus values, as seen in Fig. 2A and B. The addition of 1.5% (w/v) PAA resulted in rheological profiles within the range of those of porcine native colonic mucus, both for $PACM_{II}$ and $PACM_{III}$ (Fig. 2C and D). It should be noted that $PACM_{III}$ exhibited higher apparent viscosity and storage modulus values than $PACM_{II}$. This can be attributed to the type of mucin contained in each sample, as this was the only difference between the two preparations.

The gel network of $PACM_{II}$ and $PACM_{III}$ was visualized in order to assess the microarchitecture of the samples and validate it against recent Cryo-SEM images of porcine native colonic mucus (Barmpatsalou et al., 2021). First, $PACM_{II}$ and $PACM_{III}$ samples without PAA were imaged. The mixture of mucins (Type II and Type III), BSA, and lipids were able to form a "loose" network, as seen in Fig. 4A and B. The addition of PAA resulted in the gradual adaptation of a "honeycomb" structure in the gel network, as illustrated in earlier Cryo-SEM images (Kim et al., 2003). $PACM_{II}$ and $PACM_{III}$ samples containing 1.5% (w/v) PAA (Fig. 4C and D) presented a gel network with characteristics similar to porcine native colonic mucus (Fig. 4E). The $PACM_{III}$ samples formed a network with pores of larger diameter compared to $PACM_{II}$ and porcine native colonic mucus. Further addition of PAA might have yielded smaller pores as previously reported (Kim et al., 2003); however it was a rather strenuous process to dissolve all the solids and produce a homogenous gel sample. Again, the difference in the gel network microarchitecture of $PACM_{II}$ and $PACM_{III}$ can be related to the purification processes that mucin Types II and III undergo, resulting in different amounts of functional group residuals in the mucin monomer, as reported elsewhere (Marczynski et al., 2021). Such functional group differences might contribute to the microarchitectural differences of $PACM_{II}$ and $PACM_{III}$ in the present study, as they allow different types of interactions with the other components. It was also shown that $PACM_{II}$ and $PACM_{III}$ samples containing 1.5% (w/v) PAA were homogenous, implying uniform distribution of the artificial mucus components (Fig. 4F and G).

4.2.2. Diffusion of FITC dextrans in porcine artificial colonic mucus (PACM). Following the structural validation of $PACM_{II}$ and $PACM_{III}$ against porcine native colonic mucus, we assessed the potential of $PACM_{II}$ and $PACM_{III}$ in discriminating between diffusion of molecules of different charges and sizes. As PAA was a key contributor to the rheological properties and gel network of $PACM_{II}$ and $PACM_{III}$, it was deemed useful to assess whether a PAA mixture containing equal amounts of PAA to $PACM_{II}$ and $PACM_{III}$, but not the other components (mucin, BSA, lipids), would capture the barrier properties of porcine native colonic mucus. If so, it would be a simpler alternative for mucus diffusion studies.

Both $PACM_{II}$ and $PACM_{III}$ could adequately capture diffusivity trends due to different charges and sizes of the FITC-dextrans (Fig. 7A and B). The diffusion of cationic 4K FITC-dextran was more restricted in $PACM_{II}$, $PACM_{III}$, and the PAA mixture than in porcine native colonic mucus. This might be related to the strong negative charge of PAA, which could result in stronger binding of the positively charged 4K FITC-dextran. Indeed, the zeta potential of $PACM_{II}$, $PACM_{III}$, and the PAA mixture was -46.2±2.7, -48.7±3.5 and -35.1±1.1, respectively (Table S1). In contrast, the zeta potential of porcine native mucus was higher, ranging from -27.1 to -25.8, suggesting weaker electrostatic interactions with the diffusing cations compared to the artificial mucus models.

The diffusivity values of FITC dextrans in $PACM_{II}$ and $PACM_{III}$ followed the trends observed for porcine native colonic mucus, with good sensitivity to charge and size differences. However, $PACM_{II}$, $PACM_{III}$, and the PAA mixture exhibited a trend towards lower diffusivity values for the FITC-dextrans on the high end of the molecular size range (Fig. 7B). This trend might stem from the more rigid network of PAA which lacks the flexibility of the native mucins (Hughes et al., 2019).

From Fig. 7A, it can be concluded that the mucin, BSA, and lipids in $PACM_{II}$ and $PACM_{III}$ are necessary to capture the diffusion profiles of FITC-dextrans in porcine native colonic mucus. The mucin, BSA, and lipids interact with the diffusing molecules physicochemically, a phenomenon that delays diffusion and decreases the diffusivity values. Especially for small, highly mobile molecules, the presence of these components is detrimental, as they do not face steric hindrance due to their small size. In molecules of higher molecular weight, the molecular size plays the key limiting role and thus diminishes the contribution of other physicochemical interactions. In these cases, a PAA mixture could be an alternative to $PACM_{II}$ and $PACM_{III}$, as it presented similar diffusivity values for the 40K and 70K FITC-dextrans. The data observed herein suggest that research focusing on delivery of large molecules (>40kDa) or drug carriers could use a simple PAA-based gel as the first choice of screening tool for mucus diffusion.

Both $PACM_{II}$ and $PACM_{III}$ showed potential in identifying key diffusivity differences among molecules of various charge and size and both could replicate trends observed for porcine native colonic mucus. However, from a sample preparation point of view, $PACM_{III}$ was more cumbersome to prepare than $PACM_{II}$. It resulted in mixtures with higher viscosity and it was particularly difficult to dissolve all solids completely, a factor which would hinder production reproducibility. Given that there were no obvious differences in the diffusivity values between $PACM_{II}$ and $PACM_{III}$, $PACM_{II}$ was selected for use in further studies.

$PACM_{II}$ was successfully validated against porcine native colonic mucus and reflected the structural properties and diffusion-related characteristics of porcine native colonic mucus (Fig. 7C).

4.3. Assessment of the impact of storage conditions on the rheological properties, gel network microarchitecture and diffusion of FITC dextrans in porcine artificial colonic mucus (PACM)

Three batches of $PACM_{II}$ were prepared independently, under the same conditions, and kept at 4 ℃ overnight to allow completion of the swelling. Equal portions of each batch were then tested under various storage conditions. All $PACM_{II}$ samples showed similar rheological behavior, independent of storage conditions (Fig. 3A and B). Støvring Mortensen et al. made similar conclusions in their assessment of various storage conditions (fresh, −20°C, or at −80°C directly or after snap freezing in liquid nitrogen, or freeze-dried and reconstituted with distilled water). They found that the various storage conditions have negligible effect on the barrier properties of porcine native jejunal mucus compared to fresh secretion (Støvring Mortensen et al., 2022). In the present study, we confirmed that the same applies to $PACM_{II}$, demonstrating the flexibility and applicability of the porcine artificial colonic mucus in routine testing. Thus, upon preparation of a $PACM_{II}$ batch and after overnight storage at 4℃, aliquots can be stored at -20℃ and thawed on the day of the analysis. Additionally, storage of $PACM_{II}$ in lyophilized aliquots substantially decreases both the weight and volume and thus contributes to lower costs of transport. The samples can be ready for experimentation upon a quick reconstitution step, followed by 10 minutes of equilibration time, providing flexibility in experimental planning, reduced costs, simple, straightforward protocols as well as circumventing the biorisks related to the use of material from biological sources.

The inter- and intra-batch variability in the rheology of the three $PACM_{II}$ batches under various storage conditions (fresh, frozen at -20℃, and freeze-dried/reconstituted with MilliQ water) was assessed to explore the homogeneity of the produced samples and the reproducibility of the preparation process. The apparent viscosity varied 2- to 3-fold among batches and the storage modulus values varied 2-fold (Fig. S3). Although not negligible, the inter-batch variability was lower than that for inter-animal. Low inter-batch variability improves experimental reproducibility, which is often severely hindered when animal models are involved (Collins and Tabak, 2014). The intra-batch variability, both in apparent viscosity values and storage modulus, was negligible (except for the apparent viscosity profile of fresh samples, where it was 2-fold). These findings suggest that homogenous samples, in which all components have been uniformly dissolved can be divided into aliquots with similar rheological properties.

The impact of the three storage conditions on the network microarchitecture of $PACM_{II}$ was assessed by Cryo-SEM imaging. As seen in Fig. 5A-I, the pore network of $PACM_{II}$ samples stored under all three conditions presents similarly sized and shaped pores, suggesting that storage conditions made no substantial changes in the gel network. Assessment of the inter-batch variability also revealed a similar gel microarchitecture for all batches (Fig. 5J and K).

The diffusion of FITC-dextrans showed limited variability in $PACM_{II}$ samples stored under various conditions. Diffusion of neutral 4K FITC-dextrans was similar to anionic ones in the $PACM_{II}$ samples, while diffusion of the cationic ones was substantially lower, under the three storage conditions. The decrease can be probably attributed to the strong electrostatic interactions between the cation and the negative charge of the $PACM_{II}$ gel. Diffusion of the neutral and anionic 40K, and the neutral 70K FITC-dextrans was similar under all three storage conditions and lower than the diffusion of the neutral and anionic 4K FITC-dextrans. Thus, storage conditions did not cause alterations in the sieving function of the gels which is responsible for the molecular size discrimination. It should be noted that although the trend towards a decrease in diffusivity values for cationic 4K FITC-dextrans compared to neutral and anionic 4K FITC dextran in porcine native colonic mucus is captured and is being presented by all $PACM_{II}$ samples, the decrease in the artificial mucus samples is more pronounced. Thus, it seems that $PACM_{II}$ samples are more sensitive to the presence of diffusing cationic molecules than the native colonic mucus. As discussed above, this is probably due to the more negative charge measured in the artificial mucus. For all other FITC-dextrans, the diffusivity values were within the variability observed for native colonic mucus (Fig. 8A and B, see shaded area). In conclusion, the storage conditions did not alter the physicochemical interaction characteristics or steric hindrance of $PACM_{II}$ samples. Similar observations have been published by Støvring Mortensen et al. (Støvring Mortensen et al., 2022), suggesting that permeation of FITC dextrans in stored porcine jejunal mucus is similar to permeation through freshly isolated porcine jejunal mucus.

5. Conclusion

The present study reports the development of an *in vitro* porcine artificial colonic mucus (PACM) model validated against native colonic mucus. The model successfully captures the key trends in the diffusion of macromolecules in native colonic mucus and discriminates between differences in charge and size of the diffusing macromolecule, proving its high predictive capacity. Samples can be stored under common laboratory storage conditions, without compromising the barrier properties of PACM. PACM can be used as a reliable, biopredictive screening tool in the early stages of drug development to elucidate drug diffusion in colonic mucus and can easily be implemented in routine experimentation, due to its simple preparation protocol and flexible storage characteristics.

CRediT authorship contribution statement

Vicky Barmpatsalou: Conceptualization, Methodology, Investigation, Formal analysis, Data curation, Writing – original draft. **Agnes Rodler:** Methodology, Investigation, Writing – review & editing. **Magdalena Jacobson:** Methodology, Writing – review & editing. **Eva Marie-Louise Karlsson:** Conceptualization, Writing – review & editing. **Betty Lomstein Pedersen:** Conceptualization, Writing – review & editing. **Christel Anna Sofie Bergström:** Conceptualization, Writing – review & editing, Funding acquisition.

Data availability

Data will be made available on request.

Acknowledgments

Funding from VINNOVA (2019-00048) is gratefully acknowledged. We thank the Umeå Centre for Electron Microscopy (UCEM) and the National Microscopy Infrastructure (NMI) for assisting with the Cryo-SEM analysis. We would also like to thank the Confocal Microscopy Platform at Swedish Agricultural University and Katarina Landberg for assistance with the FRAP experiments. Prof. Per Hansson and the Department of Medicinal Chemistry are kindly acknowledged for providing access to the rheometer and the freeze drier, respectively.

Supplementary materials

Supplementary material associated with this article can be found, in the online version, at doi:10.1016/j.ejps.2022.106361.

References

Agostini, P.d.S., Manzanilla, E.G., de Blas, C., Fahey, A.G., da Silva, C.A., Gasa, J., 2015. Managing variability in decision making in swine growing-finishing units. Ir. Vet. J. 68, 20.

Ambort, D., Johansson, M.E.V., Gustafsson, J.K., Ermund, A., Hansson, G.C., 2012. Perspectives on mucus properties and formation—lessons from the biochemical world. Cold Spring Harb. Perspect. Med. 2, a014159.

Ambort, D., van der Post, S., Johansson, M.E., Mackenzie, J., Thomsson, E., Krengel, U., Hansson, G.C., 2011. Function of the CysD domain of the gel-forming MUC2 mucin. Biochem. J. 436, 61–70.

Araújo, F., Martins, C., Azevedo, C., Sarmento, B., 2018. Chemical modification of drug molecules as strategy to reduce interactions with mucus. Adv. Drug Deliv. Rev. 124, 98–106.

Atuma, C., Strugala, V., Allen, A., Holm, L., 2001. The adherent gastrointestinal mucus gel layer: thickness and physical state in vivo. Am. J. Physiol. Gastrointest. Liver Physiol. 280, G922–G929.

Bansil, R., Turner, B.S., 2006. Mucin structure, aggregation, physiological functions and biomedical applications. Curr. Opin. Colloid Interface Sci. 11, 164–170.

Barmpatsalou, V., Dubbelboer, I.R., Rodler, A., Jacobson, M., Karlsson, E., Pedersen, B.L., Bergström, C.A.S., 2021. Physiological properties, composition and structural profiling of porcine gastrointestinal mucus. Eur. J. Pharm. Biopharm. 169, 156–167.

Bernkop-Schnürch, A., Fragner, R., 1996. Investigations into the diffusion behaviour of polypeptides in native intestinal mucus with regard to their peroral administration. Pharm. Pharmacol. Commun. 2, 361–363.

Bhat, P.G., Flanagan, D.R., Donovan, M.D., 1996. Drug binding to gastric mucus glycoproteins. Int. J. Pharm. 134, 15–25.

Birch, D., Diedrichsen, R.G., Christophersen, P.C., Mu, H., Nielsen, H.M., 2018. Evaluation of drug permeation under fed state conditions using mucus-covered Caco-2 cell epithelium. Eur. J. Pharm. Sci. 118, 144–153.

Bode, G., Clausing, P., Gervais, F., Loegsted, J., Luft, J., Nogues, V., Sims, J., 2010. The utility of the minipig as an animal model in regulatory toxicology. J. Pharmacol. Toxicol. Methods 62, 196–220.

Boegh, M., Baldursdóttir, S.G., Müllertz, A., Nielsen, H.M., 2014. Property profiling of biosimilar mucus in a novel mucus-containing in vitro model for assessment of intestinal drug absorption. Eur. J. Pharm. Biopharm. 87, 227–235.

Boegh, M., García-Díaz, M., Müllertz, A., Nielsen, H.M., 2015. Steric and interactive barrier properties of intestinal mucus elucidated by particle diffusion and peptide permeation. Eur. J. Pharm. Biopharm. 95, 136–143.

Braeckmans, K., Peeters, L., Sanders, N.N., De Smedt, S.C., Demeester, J., 2003. Three-dimensional fluorescence recovery after photobleaching with the confocal scanning laser microscope. Biophys. J. 85, 2240–2252.

Brandl, F., Kastner, F., Gschwind, R.M., Blunk, T., Teßmar, J., Göpferich, A., 2010. Hydrogel-based drug delivery systems: comparison of drug diffusivity and release kinetics. J. Control. Release 142, 221–228.

Brieland, J.K., Jackson, C., Menzel, F., Loebenberg, D., Cacciapuoti, A., Halpern, J., Hurst, S., Muchamuel, T., Debets, R., Kastelein, R., Churakova, T., Abrams, J., Hare, R., O'Garra, A., 2001. Cytokine networking in lungs of immunocompetent mice in response to inhaled Aspergillus fumigatus. Infect. Immun. 69, 1554–1560.
Button, B., Okada, S.F., Frederick, C.B., Thelin, W.R., Boucher, R.C., 2013. Mechanosensitive ATP release maintains proper mucus hydration of airways. Sci. Signal 6, ra46.
Carlstedt, I., Sheehan, J.K., 1984. Macromolecular properties and polymeric structure of mucus glycoproteins. In: Ciba Foundation symposium, 109, pp. 157–172.
Carlstedt, I., Sheehan, J.K., 1989. Structure and macromolecular properties of cervical mucus glycoproteins. Symp. Soc. Exp. Biol. 43, 289–316.
Chen, E.Y.T., Wang, Y.-C., Chen, C.-S., Chin, W.-C., 2010. Functionalized positive nanoparticles reduce mucin swelling and dispersion. PLoS One 5, e15434.
Cobarrubia, A., Tall, J., Crispin-Smith, A., Luque, A., 2021. Empirical and theoretical analysis of particle diffusion in mucus. Front. Phys. 9.
Colleton, C., Brewster, D., Chester, A., Clarke, D.O., Heining, P., Olaharski, A., Graziano, M., 2016. The use of minipigs for preclinical safety assessment by the pharmaceutical industry: results of an IQ DruSafe Minipig Survey. Toxicol. Pathol. 44, 458–466.
Collins, F.S., Tabak, L.A., 2014. Policy: NIH plans to enhance reproducibility. Nature 505, 612–613.
Cone, R.A., 2009. Barrier properties of mucus. Adv. Drug Deliv. Rev. 61, 75–85.
Crater, J.S., Carrier, R.L., 2010. Barrier properties of gastrointestinal mucus to nanoparticle transport. Macromol. Biosci. 10, 1473–1483.
Curt, J.R., Pringle, R., 1969. Viscosity of gastric mucus in duodenal ulceration. Gut 10, 931–934.
Desai, M.A., Mutlu, M., Vadgama, P., 1992. A study of macromolecular diffusion through native porcine mucus. Experientia 48, 22–26.
Desai, M.A., Vadgama, P., 1991. Estimation of effective diffusion coefficients of model solutes through gastric mucus: assessment of a diffusion chamber technique based on spectrophotometric analysis. Analyst 116, 1113–1116.
Dubbelboer, I.R., Barmpatsalou, V., Rodler, A., Karlsson, E., Nunes, S.F., Holmberg, J., Häggström, J., Bergström, C.A.S., 2022. Gastrointestinal mucus in dog: physiological characteristics, composition, and structural properties. Eur. J. Pharm. Biopharm. 173, 92–102.
Falavigna, M., Klitgaard, M., Berthelsen, R., Müllertz, A., Flaten, G.E., 2021. Predicting oral absorption of fenofibrate in lipid-based drug delivery systems by combining in vitro lipolysis with the mucus-pvpa permeability model. J. Pharm. Sci. 110, 208–216.
Fröhlich, E., Roblegg, E., 2014. Mucus as barrier for drug delivery by nanoparticles. J. Nanosci. Nanotechnol. 14, 126–136.
Griffiths, P.C., Cattoz, B., Ibrahim, M.S., Anuonye, J.C., 2015. Probing the interaction of nanoparticles with mucin for drug delivery applications using dynamic light scattering. Eur. J. Pharm. Biopharm. 97, 218–222.
Henze, L.J., Koehl, N.J., O'Shea, J.P., Kostewicz, E.S., Holm, R., Griffin, B.T., 2019. The pig as a preclinical model for predicting oral bioavailability and in vivo performance of pharmaceutical oral dosage forms: a PEARRL review. J. Pharm. Pharmacol. 71, 581–602.
Huck, B.C., Hartwig, O., Biehl, A., Schwarzkopf, K., Wagner, C., Loretz, B., Murgia, X., Lehr, C.M., 2019. Macro- and microrheological properties of mucus surrogates in comparison to native intestinal and pulmonary mucus. Biomacromolecules 20, 3504–3512.
Hughes, G.W., Ridley, C., Collins, R., Roseman, A., Ford, R., Thornton, D.J., 2019. The MUC5B mucin polymer is dominated by repeating structural motifs and its topology is regulated by calcium and pH. Sci. Rep. 9, 17350.
Iqbal, J., Shahnaz, G., Dünnhaupt, S., Müller, C., Hintzen, F., Bernkop-Schnürch, A., 2012. Preactivated thiomers as mucoadhesive polymers for drug delivery. Biomaterials 33, 1528–1535.
Johansson, M.E.V., Phillipson, M., Petersson, J., Velcich, A., Holm, L., Hansson, G.C., 2008. The inner of the two Muc2 mucin-dependent mucus layers in colon is devoid of bacteria. Proc. Natl. Acad. Sci. 105, 15064–15069.
Kim, J.-Y., Song, J.-Y., Lee, E.-J., Park, S.-K., 2003. Rheological properties and microstructures of Carbopol gel network system. Colloid. Polym. Sci. 281, 614–623.
Kocevar-Nared, J., Kristl, J., Smid-Korbar, J., 1997. Comparative rheological investigation of crude gastric mucin and natural gastric mucus. Biomaterials 18, 677–681.
Lai, S.K., Wang, Y.-Y., Wirtz, D., Hanes, J., 2009. Micro- and macrorheology of mucus. Adv. Drug Deliv. Rev. 61, 86–100.
Larhed, A.W., Artursson, P., Björk, E., 1998. The influence of intestinal mucus components on the diffusion of drugs. Pharm. Res. 15, 66–71.
Larhed, A.W., Artursson, P., Gråsjö, J., Björk, E., 1997. Diffusion of drugs in native and purified gastrointestinal mucus. J. Pharm. Sci. 86, 660–665.
Li, Leon D., Crouzier, T., Sarkar, A., Dunphy, L., Han, J., Ribbeck, K., 2013. Spatial configuration and composition of charge modulates transport into a mucin hydrogel barrier. Biophys. J. 105, 1357–1365.
Lim, Y.F., Williams, M.A.K., Lentle, R.G., Janssen, P.W.M., Mansel, B.W., Keen, S.A.J., Chambers, P., 2013. An exploration of the microrheological environment around the distal ileal villi and proximal colonic mucosa of the possum (*Trichosurus vulpecula*). J. R. Soc. Interface 10, 20121008.
Lindén, S., Nordman, H., Hedenbro, J., Hurtig, M., Borén, T., Carlstedt, I., 2002. Strain- and blood group-dependent binding of Helicobacter pylori to human gastric MUC5AC glycoforms. Gastroenterology 123, 1923–1930.
Macierzanka, A., Mackie, A.R., Krupa, L., 2019. Permeability of the small intestinal mucus for physiologically relevant studies: impact of mucus location and ex vivo treatment. Sci. Rep. 9, 17516.
Madsen, F., Eberth, K., Smart, J.D., 1998. A rheological assessment of the nature of interactions between mucoadhesive polymers and a homogenised mucus gel. Biomaterials 19, 1083–1092.
Marczynski, M., Jiang, K., Blakeley, M., Srivastava, V., Vilaplana, F., Crouzier, T., Lieleg, O., 2021. Structural alterations of mucins are associated with losses in functionality. Biomacromolecules 22, 1600–1613.
Meldrum, O.W., Yakubov, G.E., Bonilla, M.R., Deshmukh, O., McGuckin, M.A., Gidley, M.J., 2018. Mucin gel assembly is controlled by a collective action of non-mucin proteins, disulfide bridges, Ca(2+)-mediated links, and hydrogen bonding. Sci. Rep. 8, 5802.
Navabi, N., McGuckin, M.A., Lindén, S.K., 2013. Gastrointestinal cell lines form polarized epithelia with an adherent mucus layer when cultured in semi-wet interfaces with mechanical stimulation. PLoS One 8, e68761.
Patterson, J.K., Lei, X.G., Miller, D.D., 2008. The pig as an experimental model for elucidating the mechanisms governing dietary influence on mineral absorption. Exp. Biol. Med. 233, 651–664.
Peng, K., Gao, Y., Angsantikul, P., LaBarbiera, A., Goetz, M., Curreri, A.M., Rodrigues, D., Tanner, E.E.L., Mitragotri, S., 2021. Modulation of gastrointestinal mucus properties with ionic liquids for drug delivery. Adv. Healthc. Mater. 10, 2002192.
Perez-Vilar, J., Hill, R.L., 1999. The structure and assembly of secreted mucins. J. Biol. Chem. 274, 31751–31754.
Riley, R.G., Smart, J.D., Tsibouklis, J., Dettmar, P.W., Hampson, F., Davis, J.A., Kelly, G., Wilber, W.R., 2001. An investigation of mucus/polymer rheological synergism using synthesised and characterised poly(acrylic acid)s. Int. J. Pharm. 217, 87–100.
Røn, T., Patil, N.J., Ajalloueian, F., Rishikesan, S., Zappone, B., Chronakis, I.S., Lee, S., 2017. Gastric mucus and mucuslike hydrogels: thin film lubricating properties at soft interfaces. Biointerphases 12, 051001.
Rowan, A.M., Moughan, P.J., Wilson, M.N., Maher, K., Tasman-Jones, C., 1994. Comparison of the ileal and faecal digestibility of dietary amino acids in adult humans and evaluation of the pig as a model animal for digestion studies in man. Br. J. Nutr. 71, 29–42.
Ruiz-Pulido, G., Medina, D.I., 2021. An overview of gastrointestinal mucus rheology under different pH conditions and introduction to pH-dependent rheological interactions with PLGA and chitosan nanoparticles. Eur. J. Pharm. Biopharm. 159, 123–136.
Sardelli, L., Pacheco, D.P., Ziccarelli, A., Tunesi, M., Caspani, O., Fusari, A., Briatico Vangosa, F., Giordano, C., Petrini, P., 2019. Towards bioinspired in vitro models of intestinal mucus. RSC Adv. 9, 15887–15899.
Sellers, L.A., Allen, A., Morris, E.R., Ross-Murphy, S.B., 1991. The rheology of pig small intestinal and colonic mucus: weakening of gel structure by non-mucin components. Biochim. Biophys. Acta 1115, 174–179.
Sigurdsson, H.H., Kirch, J., Lehr, C.M., 2013. Mucus as a barrier to lipophilic drugs. Int. J. Pharm. 453, 56–64.
Støvring Mortensen, J., Saaby, L., Harloff-Helleberg, S., Mørck Nielsen, H., 2022. Barrier properties of ex vivo porcine intestinal mucus are highly independent of isolation and storage conditions. Eur. J. Pharm. Biopharm. 174, 106–110.
Swindle, M.M., Makin, A., Herron, A.J., Clubb, F.J., Frazier, K.S., 2012. Swine as models in biomedical research and toxicology testing. Vet. Pathol. 49, 344–356.
Thornton, D.J., Sheehan, J.K., 2004. From mucins to mucus: toward a more coherent understanding of this essential barrier. Proc. Am. Thorac. Soc. 1, 54–61.
van der Laan, J.W., Brightwell, J., McAnulty, P., Ratky, J., Stark, C., 2010. Regulatory acceptability of the minipig in the development of pharmaceuticals, chemicals and other products. J. Pharmacol. Toxicol. Methods 62, 184–195.
Wright, L., Joyce, P., Barnes, T.J., Prestidge, C.A., 2021. Mimicking the gastrointestinal mucus barrier: laboratory-based approaches to facilitate an enhanced understanding of mucus permeation. ACS Biomater. Sci. Eng. epub ahead of print Nov 16.
Yildiz, H.M., McKelvey, C.A., Marsac, P.J., Carrier, R.L., 2015. Size selectivity of intestinal mucus to diffusing particulates is dependent on surface chemistry and exposure to lipids. J. Drug Target. 23, 768–774.